

# DOE Study of Epitaxial Layer Thickness and Resistivity Effects on P-i-N Diode for beyond 300 V of Reverse Voltage Applications

J. H. See<sup>1</sup>, M. K. Md Arshad<sup>1,2</sup>, M. F. M. Fathil<sup>1</sup>, C. H Voon<sup>1</sup>, U. Hashim<sup>1,2</sup>, Subash C. B. Gopinath<sup>1</sup>

<sup>1</sup>Institute of Nano Electronic Engineering, Universiti Malaysia Perlis, Kangar, Perlis, Malaysia

<sup>2</sup>School of Microelectronic Engineering, Universiti Malaysia Perlis, Kangar, Perlis, Malaysia

**Abstract:** A discrete power switching device used in the applications of computer and telecommunications requires operating less than 300 V during reverse bias, but for the use of motor control, robotics, and power distribution, it requires operating at beyond 300 V. With the current design structure, the P-i-N diode device can only operate at 250 V. To widen the operating range of the P-i-N power switching avalanche diode that can be operated more than 300 V, we studied the effects of the epitaxial layer thickness (WD) and resistivity ( $\rho$ ) during forward and reverse biasing by performing a process simulation as well as the confirmation on the two level factorials of design of experiment (DOE) of physical wafers. The result shows that, the changes of the WD of 42  $\mu\text{m}$  and  $\rho$  of 32 ohm-cm on a P-i-N diode can increase the reverse breakdown voltage (VR) performance beyond 300 V during reverse bias.

**Keywords:** Forward voltage; Breakdown voltage; Power device

## Načrtovanje eksperimenta vplivov debeline in upornosti epitaksijske plasti P-i-N diode pri reverzних napetostih nad 300 V

**Izveček:** Diskretni močnostni stikalni element za uporabo v računalnikih in telekomunikacijah zahteva delovanja pri zaporni napetosti pod 300 V. Pri krmiljenju motorjev, v robotiki ali pri močnostnih aplikacijah pa zahteva delovanje v zaporni smeri preko 300 V. Trenutna struktura P-i-N diode lahko deluje le do 250 V. Za višje napetosti je potrebna močnostna plazovita P-i-N dioda, na kateri smo preučevali vplive debeline epitaksijske plasti in upornosti pri prevodni in zaporni napetosti. Analiza sloni na simulaciji procesa dvonivojske faktorizacije načrtovanja eksperimenta silicijeve rezine. Rezultati izkazujejo, da sprememba debeline za 42  $\mu\text{m}$  in upornosti za 32 ohm-cm zviša prebojno napetost preko 300 V.

**Ključne besede:** Forward voltage; Breakdown voltage; Power device

\*Corresponding Author's e-mail: mohd.khairuddin@unimap.edu.my

### 1 Introduction

Diode is a simple semiconductor device with two terminals, allowing only unidirectional current to flow. It is created with the presence of p-type and n-type semiconductor materials in intimate contact on an atomic scale, yielding the P-N junction in between [1]. The formation of P-N junction occurred by diffusion of acceptor impurities (p-type dopant) into an n-type silicon crystal or vice versa. A depletion region formed instantaneously across a P-N junction and it is easily to be described when the junction is in thermal equilibrium or

in a steady state: in both of these cases, the properties of the system does not vary in time; thus, it is known as dynamic equilibrium [2, 3]. Figure 1 (a) shows the diode 2D structure and electrical field distribution of P-N diode. For high power applications, an ideal power diode should be able of conducting high forward bias current ( $I_F$ ) during forward bias voltage ( $V_F$ ) of  $\sim 0.7$  V and supporting high reverse breakdown voltage ( $V_R$ ) in the range of 50 to 200 V [4, 5].

During reverse bias, P-N diode experiences the avalanche breakdown. To achieve the avalanching, besides the requirement of a large field, it also requires a sufficient distance to allow the electron to accelerate, hence gain enough kinetic energy, and lead to an avalanche of multiple hole-electron pair's creation [6]. In other words, to ensure the high  $V_R$ , a thick n-type substrate bulk is required for a vertical structure of simple P-N junction diode. For a vertical structure of P-N junction diode, a very thick wafer substrate bulk can be used to fulfill the requirement of a power diode. However, thicker substrate exhibits several drawbacks, which are 1) greater weight and 2) higher production cost.

Alternatively, higher  $V_R$  and  $I_F$  can be achieved by using the P-i-N diode structure with a thinner substrate. The P-i-N diode was one of the very first semiconductor devices developed for power circuit application [4, 7]. This evolution came from a conventional P-N junction diode with the addition of an extra intrinsic layer deposited between p-type and n-type regions. Figure 1 (b) (i) illustrates the P-i-N diode structure in 2D structure and electrical field distribution of P-i-N diode. In P-i-N diode, the reverse breakdown voltage is dependence on the depletion region formed with a P-N junction structure. The voltage is primary determined within the N-type drift region. Thus low doping concentration for the N-type drift region is more beneficial in order to hold the carrier from flowing between P- and N-region. The silicon P-i-N diode is designed to support large voltages, which rely upon the high level injection of minority carrier in the N-type drift region [8]. Therefore, to support a large voltage in the reverse breakdown voltage mode, an appropriate choice of doping concentration and thickness of the N-drift region needs to be made. Nevertheless, a narrower drift region is preferable because it can contain smaller amount of stored charges during the on-state operation, enabling faster turn-off.

Material substitution is one way to achieve narrower drift region thickness [9]. For example, by using silicon carbide, narrower drift region can be attained when compared to silicon devices. This is due to much larger electric field can be supported in silicon carbide. As a result, it favors a faster switching speed with reduced reverse recovery current and very high breakdown voltage can be achieved [10]. However, the high cost is a major concern, and silicon P-i-N diode still can be modified and continue to play an important role in the application, especially in medium range of breakdown voltage.

This can be explained based on expression as shown in Equation (2). The expression for  $V_R$  in this P-i-N diode can be derived by using higher critical electric field ( $E_C$ ) [11, 12] Based on Figure 1 (b) (ii),  $E_C$  is the critical elec-

tric field and  $W_D$  is depletion region thickness during reverse bias. Since P-i-N diode operates in a thickness-limited mode, which is controlled by the thickness of N- region epitaxial layer, the  $W_D$  can be referred to as the thickness of the N- epitaxial layer in i-region. The  $V_R$  can be calculated as the area of the trapezium (Figure 1 (b) (ii)) as in Equation (2).

$$V_R = \frac{1}{2} (E_C + E_1) W_D \tag{2}$$

By using the Equation (2) for the variation in the electric field with distance:

$$E_1 = E_C - \frac{q N_D}{\epsilon_S} W_D \tag{3}$$

and substituting Equation (3) in Equation (2), the  $V_R$  for the punch through diode is obtained as in Equation (4):

$$V_R = E_C W_D - \frac{q N_D W_D^2}{2 \epsilon_S} \tag{4}$$

The  $V_R$  can be affected by the variable thickness of the N- region ( $W_D$ ) and the doping concentration of the N-

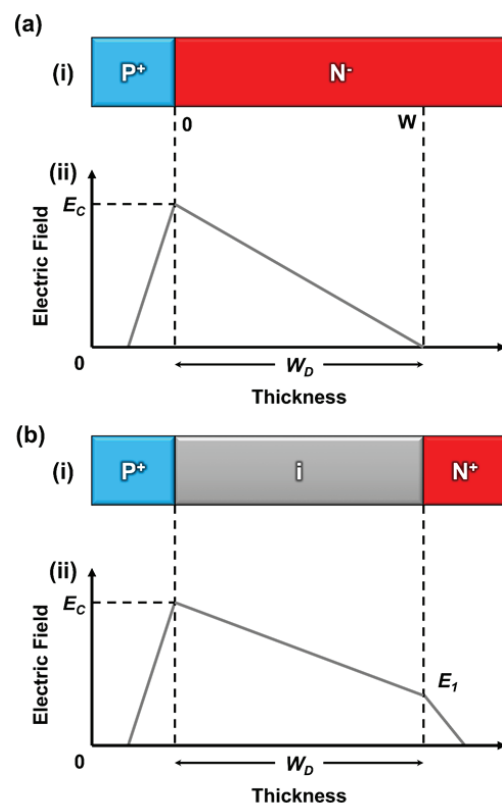


**Figure 1:** Comparison of ideal (a) P-N junction and (b) P-i-N diode in terms of (i) 2D structure and (ii) electrical field distribution.

epitaxial layer ( $N_D$ ). The  $N_D$  can be translated into the resistivity of the N- layer [11]. The increase of the  $N_D$  results in lower resistivity.

In this paper, P-i-N diode with high resistivity N region (N- region) is used to replace the intrinsic layer. For this purpose, a commercially available 250 V P-i-N power switching diode was used to evaluate effects of N- epitaxial layer thickness ( $W_D$ ) and resistivity ( $\rho$ ) as the intrinsic layer effect to the P-i-N power switching diode on the performance of current-voltage (I-V) characteristic in terms of diode's  $V_R$ . The aim of this study is to have a diode that can withstand beyond 250 V for motor control, robotics and power distribution applications. The N- region is deposited on top of the wafer substrate through epitaxial process.

## 2 Methodology

In this work, the simulation of the P-i-N diode is performed using technology computer-aided design (TCAD) simulation software i.e. Sentaurus WorkBench, as well as the fabrication and characterization of the P-i-N diode. The P-i-N power switching diode diffuses a circular shaped boron (P+ anode junction) into an N- type epitaxial layer on a low bulk resistance N+ substrate. Another N+ diffused isolation region at the perimeter of the anode junction to reduces leakage current. The backside of the wafer is sputtered with platinum (Pt) and gold (Au). The process followed by a quick drive-in cycle for both elements, from the bulk all the way through the epitaxial layer and the P+ anode junction. Pt improves the life time cycle, reducing the reverse recovery time ( $t_{rr}$ ) [13]. Au increases the epitaxial layer's  $t_{rr}$  resistance, which increases the resistance of drastic oscillation of the signal. Thus, it produces a wider P-N junction depletion region and reducing the capacitance. Figure 2 illustrates the cross-section design of the P-i-N power switching diode.

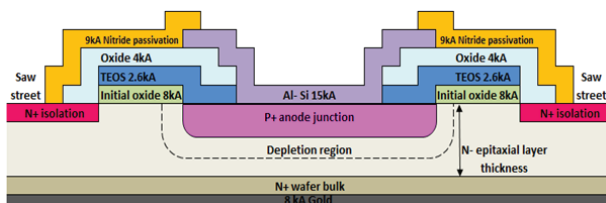


**Figure 2:** Cross-section structure of P-i-N power switching diode.

### 2.1 Numerical Simulation

The  $V_R$  of P-i-N power switching diode operates in  $W_D$  limited mode of the epitaxial layer. The first approach

is to alter the  $W_D$  by adjusting the depth of the P+ anode junction through diffusion with boron as demonstrated in Figure 2. By reducing the junction diffusion drive time, a shallower anode junction is formed. With this approach, the  $W_D$  is increased [14]. However, this method has several weaknesses. The anode junction diffusion process is difficult to control, which leads to process variation. The inconsistent process temperature of diffusion furnace results in lower  $V_R$  at the edges compared to the centre of the wafers, as wafer edges tend to have a higher process temperature compared to the wafer centre [14]. Another drawback is the diffusion process is performed under a high temperature, thus caused the up diffusion from the heavily doped N+ bulk substrate. This resulted in a less favourable higher  $V_F$  [14].

The second approach is to adjust the epitaxial layer profile ( $W_D$  and  $\rho$ ) of the substrate [14]. With the zero punch through structure of the P-i-N diode, as observed from the Equation (4), the  $W_D$  and  $N_D$  are dominant factors, which increase the  $V_R$ . The second approach is more favourable due to better control of wafer fabrication process.

A series of simulation and DOE is performed to show the effects of the  $W_D$  and  $N_D$  on the I-V characteristic using TCAD simulation software. The applications of TCAD simulation include technology and design rule development, as well as the extraction of compact models for manufacturability [15]. Initially, a half diode cross-section structure is designed by using SProcess. After the half diode is created, reflecting boundary conditions is applied to generate a full simulation diode model symmetrically.

For the SProcess step, a layer of phosphorus dopant (N- epitaxial) thickness is grown on top of the N+ bulk silicon substrate, which is initially doped with arsenic. The silicon substrate orientation of  $\langle 100 \rangle$  is used. The dopant parameter is defined as @epidose@ and  $W_D$  parameter is defined as @epiThick@. With the parameters are defined in general, several  $W_D$  and doping concentrations are utilized in the simulation (Table 1) to evaluate the output response of the I-V characteristic.

**Table 1:** Simulation thickness and concentration dosage of N- layer.

Split	Epitaxial Layer Thickness, @epiThick@ ( $\mu\text{m}$ )	Epitaxial Layer Dopant Concentration, @epidose@ ( $\text{cm}^{-3}$ )
a	42	$1.68 \times 10^{14}$
b	42	$1.58 \times 10^{14}$
c	42	$1.48 \times 10^{14}$
d	42	$1.36 \times 10^{14}$

e	34	$1.68 \times 10^{14}$
f	34	$1.58 \times 10^{14}$
g	34	$1.48 \times 10^{14}$
h	34	$1.36 \times 10^{14}$

The selection of the 34  $\mu\text{m}$  and 42  $\mu\text{m}$  thickness of  $W_D$  in simulation is due to lower and upper specification on the existing diode device epitaxial layer evaluation shown as group C in Figure 5, which will be explained in Section 2.2. The various dopant concentrations of N- epitaxial layer are selected to measure the electrical output response impact in simulation. By adjusting the phosphorus dopant concentration at the N- epitaxy layer via implantation, the  $\rho$  can be controlled, since the dopant concentration is inversely proportional with resistivity [16].

Subsequently, a 1  $\mu\text{m}$  thickness of oxide layer is deposited, followed by opening of the anode area with the photolithography and etching process for electrode deposition. Next, boron is implanted with a dosage of  $5 \times 10^{15} \text{ cm}^{-3}$ , anode junction drive in temperature and time for 1200  $^\circ\text{C}$  and 240 mins, respectively. After the anode junction is formed, the oxide layer is stripped off and then re-deposited with the same thickness. This re-deposited oxide layer is to react as the pattern oxide, followed by a 2  $\mu\text{m}$  thickness of front metal Al layer, which act as the ohmic contact and a 1  $\mu\text{m}$  thickness of  $\text{Si}_3\text{N}_4$  nitride layer, which act as the passivation layer. All of these three layers are formed with photolithography and etching process. The final device structure is shown in Figure 3.

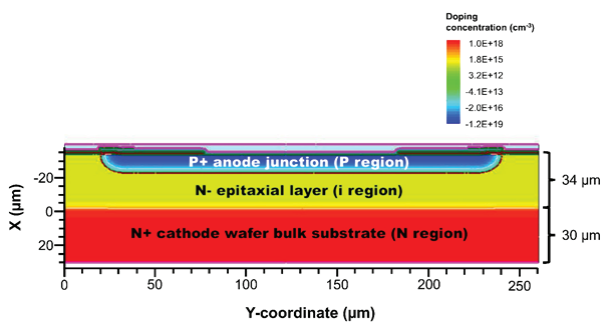


**Figure 3:** P-i-N diode structure with doping profile distribution.

### 2.2 Design of experiment and process split

Based on the simulated results, the devices are fabricated with a four corners matrix DOE to investigate the effects of  $W_D$  and  $\rho$  in order to achieve  $V_R$  above 300 V. In the fabrication process, the epitaxial layer is grown and diffused with dopant material on the wafer bulk as shown in Figure 4.

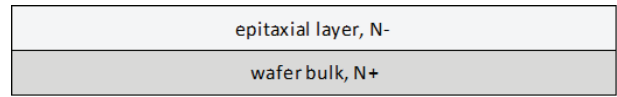


**Figure 4:** Wafer starting material with deposited epitaxial layer.

The DOE of the four corners matrix that includes the  $W_D$  and  $\rho$  is detailed in Table 2. As mentioned previously, the epitaxial layer dopant concentration and  $\rho$  are inter-related. The relationship between resistivity and phosphorus doping concentration has been studied for doped silicon as in [16]. Four corners matrix are groups of epitaxial layer covering the lower and upper specifications. It is used in the evaluation of the P-i-N diode performance when operating at the corners (lower or upper end) of epitaxial specifications as compared to the centre. Illustrations of total 5 groups with two level factorial DOE are shown in Figure 5 consisting of group A, B, C, D and E. The two factors (epitaxial layer thickness and resistivity) in low, centre and high condition. Design of experiments (DOE) is a systematic approach

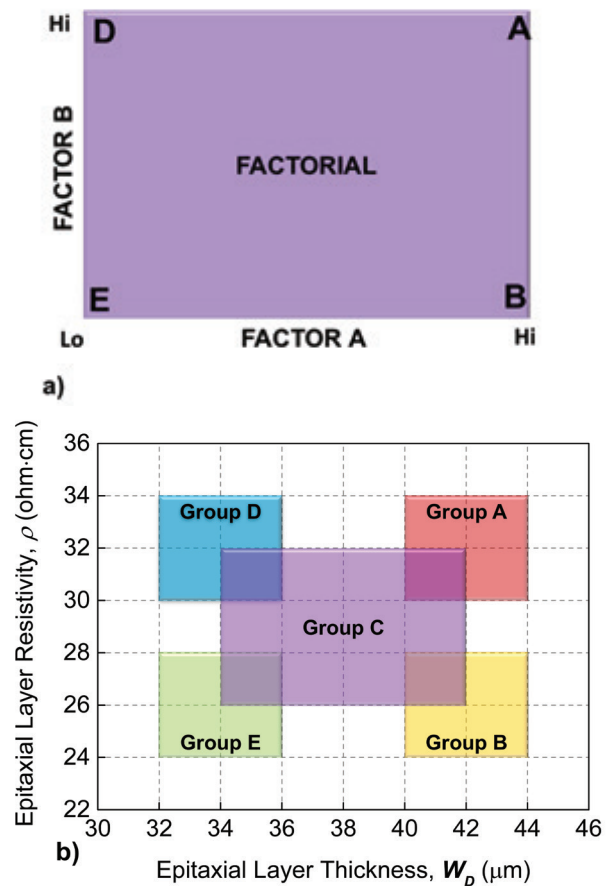


**Figure 5:** a) Two level factorials of DOE, Factor A and B refer to epitaxial layer thickness and epitaxial layer resistivity respectively. b) The location of four corners and centre of the evaluation samples consists of group A, B, C, D and E.

in engineering problem-solving that applies principles and techniques from the data collection stage. The output response from the data collection includes forward voltage, reverse breakdown voltage and reverse leakage current. The focus on the study is to increase the  $V_R$  during reverse bias without changing much of the  $V_F$  and  $I_R$ .

A total of 15 wafers lot are fabricated with the same P-i-N diode design at process corners with low/high  $W_D$  and low/high  $p$ . Afterward, the wafers are fabricated and electrically characterized. Electrical results of  $V_F$ ,  $V_R$ , and reverse leakage current ( $I_R$ ) are the main parameters of interest and then analysed with statistical software (for profiler study). The predicted profiler study is done to determine the dominant factor that affects the electrical performance and the optimal epitaxial profile. To ensure the repeatability of the result, each of the splits is repeated 3 times for the wafer fabrication and characterization.

### 3 Results and discussions

#### 3.1 Simulation results

Figure 6 shows (a) reverse bias and (b) forward bias of the simulated I-V characteristics for different  $W_D$  and

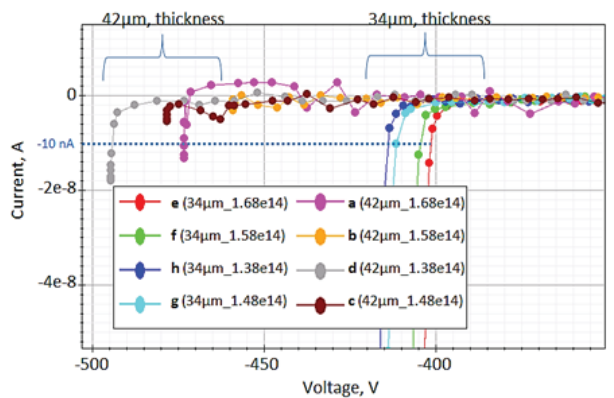
concentration of the N- epitaxial layer as tabulated in Table 1. In Figure 6 (a), a clear significant difference of the  $V_R$  with difference of  $W_D$  (i.e. 34 and 42  $\mu\text{m}$ ) is observed. At 10 nA (shown as dotted line), the 34  $\mu\text{m}$  of  $W_D$  results in lower  $V_R$  ranging from -400 V to -415 V. In contrast the 42  $\mu\text{m}$  of  $W_D$  shows a higher  $V_R$  ranging from 460 V to 490 V. The increase of the  $W_D$  leads to an increment of the stored charges available and makes the diode to behave like a resistor [17]. According to Ohm's law and with the same current, the resistance is increased as a result of the increase in voltage. On the other hand, the increase of the dopant concentration  $N_D$  from  $1.38 \times 10^{14} \text{ cm}^{-3}$  to  $1.68 \times 10^{14} \text{ cm}^{-3}$ , results in slight decrease of  $V_R$ . This shows that the  $W_D$  is more dominance factor affecting the  $V_R$  performance. Nevertheless, both impacts are in agreement with Equation (4) as previously explained.

Figure 6 (b) shows the forward bias results of the simulated diode. One can see that, significant impact is only related to the different  $W_D$  (i.e. 34  $\mu\text{m}$  and 42  $\mu\text{m}$ ), while no variation can be observed for different dopant concentration. In comparison between 34  $\mu\text{m}$  and 42  $\mu\text{m}$  of  $W_D$ , 1) at low current of 200 mA (shown in the blue dotted line) regardless of the dopant concentration difference,  $V_F$  values of 870 mV and 880 mV, respectively. At low  $I_F$  biasing, the difference of the  $W_D$  results in a small change of  $V_F$  with the range of 10 mV difference. 2) The difference in  $V_F$  output response becomes widen

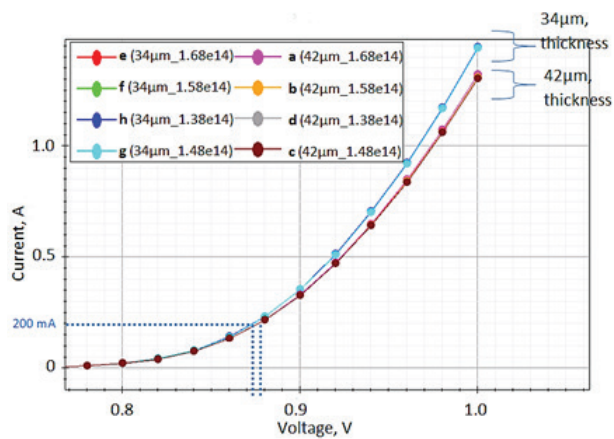
**Table 2:** Substrate 4 corner split table

Wafer#	Group	Description (Thickness/ Resistivity)	Target Thickness ( $\mu\text{m}$ )	Phosphorus dopant concentration ( $\text{cm}^{-3}$ )	Conversion of dopant concentration to Resistivity (ohm-cm)	Target resistivity value (ohm-cm)	Exact Thickness value ( $\mu\text{m}$ )	Exact resistivity value (ohm-cm)
1	A	High / High	42	$1.36 \times 10^{14}$	32.8	32	42.6	33.223
2	D	Low / High	34	$1.36 \times 10^{14}$	32.8	32	34.34	30.093
3	C	Center / Center	38	$1.58 \times 10^{14}$	28.2	29	37.95	28.742
4	A	High / High	42	$1.36 \times 10^{14}$	32.8	32	42.6	33.223
5	D	Low / High	34	$1.36 \times 10^{14}$	32.8	32	34.34	30.093
6	B	High / Low	42	$1.68 \times 10^{14}$	26.6	26	42.15	26.524
7	E	Low / Low	34	$1.68 \times 10^{14}$	26.6	26	33.85	25.723
8	C	Center / Center	38	$1.58 \times 10^{14}$	28.2	29	37.89	28.742
9	B	High / Low	42	$1.68 \times 10^{14}$	26.6	26	42.15	26.524
10	E	Low / Low	34	$1.68 \times 10^{14}$	26.6	26	33.85	25.723
11	A	High / High	42	$1.36 \times 10^{14}$	32.8	32	42.6	33.223
12	C	Center / Center	38	$1.58 \times 10^{14}$	28.2	29	37.95	28.742
13	D	Low / High	34	$1.36 \times 10^{14}$	32.8	32	34.34	30.093
14	E	Low / Low	34	$1.68 \times 10^{14}$	26.6	26	33.85	25.723
15	B	High / Low	42	$1.68 \times 10^{14}$	26.6	26	42.15	26.524

between various  $W_D$  with the increase of the  $I_F$ . This can be explained, when a P-i-N diode is forward biased, where holes and electrons are injected from the P and N regions into the i-region, which is represented as  $W_D$ . These charges do not recombine immediately. Instead, a finite quantity of charge always remains stored and results in a lowering of the  $\rho$ . So, the increase of  $I_F$  leads the decrease of the forward series resistance ( $R_s$ ) [18]. The  $W_D$  plays a greater role to change the  $V_F$  with low resistivity.



(a)



(b)

**Figure 6:** I-V characteristics under (a) reverse bias and (b) forward bias for different  $W_D$  and dopant concentrations.

From the simulation, by changing the  $W_D$  and dopant concentration of the epitaxial layer, the  $V_R$  shows more significant difference compared to  $V_F$ . The reason being the P-i-N diode exhibiting reverse capacitance characteristics during reverse bias where dopant concentration and the  $W_D$  shows a more responsive curve. While forward biasing, P-i-N diode exhibits the forward series resistance characteristics where the difference of the  $W_D$  plays a greater role when the  $I_F$  is increased to a certain level [18], [19]. The phenomenon of the less responsive output on the forward bias is preferable as the focus on the study is to increase the  $V_R$  during reverse bias without changing the  $V_F$ .

With the confirmation of the theory through the TCAD simulation software, a wafer fabrication DOE has been conducted to validate the results by taking into account of the process variation and material variation.

### 3.2 DOE wafer results

From the DOE experimental results, in addition to  $V_R$  and  $V_F$  and  $I_R$  are also considered. The statistical analysis, i.e. JMP profiler is used to analyse the effect of the  $W_D$  and  $\rho$  as shown in Figure 7. The line curve can be analysed by separating the two groups, which are  $W_D$  and  $\rho$  versus electrical responses. The x-axis of the chart represents the  $W_D$ , the  $\rho$  and the desirability of the responses. The curvature of the line in desirability row indicates how impactful the two factors ( $W_D$  and  $\rho$ ) to the electrical output response of the device. The y-axis represents the electrical output response of  $V_R$ ,  $V_F$  and  $I_R$ .

In Figure 7,  $W_D$  plays a dominant factor compared to the  $\rho$  in  $V_R$  and  $V_F$ . This is due to the  $V_R$  and  $V_F$  show more responsive curve on  $W_D$  compared to  $\rho$ . In other words, a greater gradient is observed in  $W_D$  line curve when compared to the  $\rho$ . However, the  $I_R$  change on both  $W_D$  and  $\rho$  is not significant (in nano-ampere range).

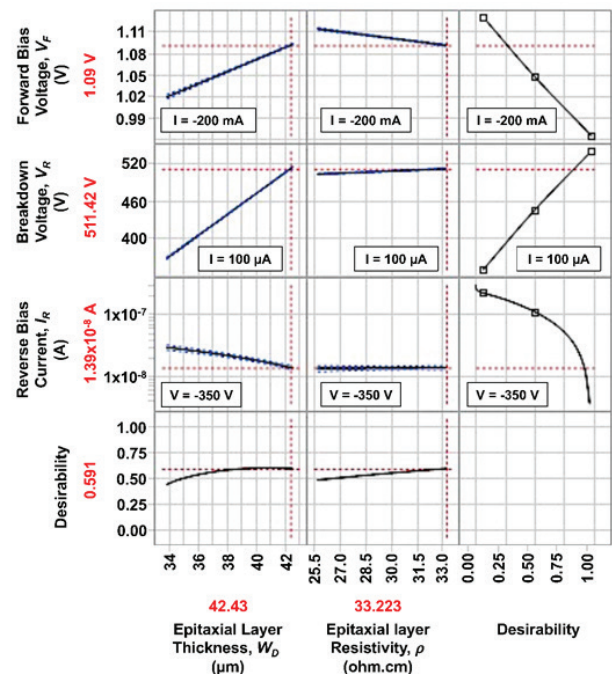


**Figure 7:** Statistical data on the impact of  $W_D$  and  $\rho$  on the fabricated devices.

As expected, by changing the  $W_D$  (34  $\mu\text{m}$  to 42  $\mu\text{m}$ ), a significant difference on electrical performance for both  $V_F$  at 200 mA and  $V_R$  at 100  $\mu\text{A}$  can be observed. This is related to the increase of the  $W_D$  results in the

$V_R$  and  $V_F$  is also increased. Interesting to note that, an increase of  $V_F$  around 10 mV can be observed in Figure 7, is similar to the result obtained in simulation Figure 6 (b). With  $W_D$  increased from 34  $\mu\text{m}$  to 42  $\mu\text{m}$ , at 100  $\mu\text{A}$ , the  $V_R$  shows almost similar response between simulations versus actual DOE. The voltage different between simulation and actual DOE is around 20 V is due to the uniformity of the boron pre deposition process.

In Figure 7, based on the statistical analysis JMP software, the  $V_R$  shows a significant improvement from 300 V to more than 500 V when replaced with  $W_D$  of 42.43  $\mu\text{m}$  and the  $\rho$  of 33.22 ohm.cm.

From the DOE evaluation, both  $W_D$  and  $\rho$  in group A shows the optimum condition to achieved the desired device performance. The target  $W_D$  is 42  $\mu\text{m}$  with window of 40–44  $\mu\text{m}$  and the target  $\rho$  is 32 ohm.cm with window of 30–34 ohm.cm. The tolerance of  $\pm 4 \mu\text{m}$  of  $W_D$  and  $\pm 2$  ohm.cm window are the narrowest tolerance, limited by process fabrication for this device. The small tolerance is preferable to reduce the process variation. With the fixed epitaxial layer substrate profile window, a total of 3 qualification lots with 5 wafers each have been fabricated in different time frames to monitor the process variation. All  $V_R$  and  $V_F$  are monitored at

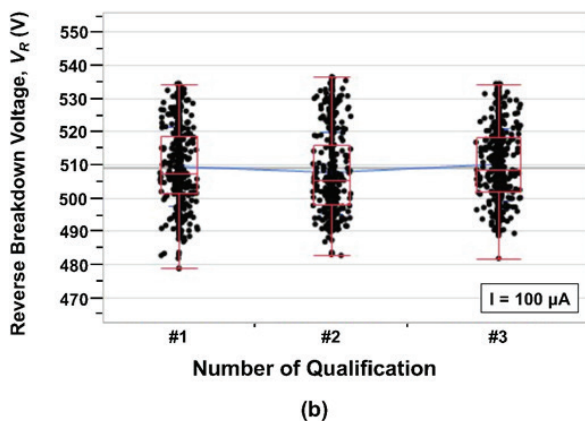
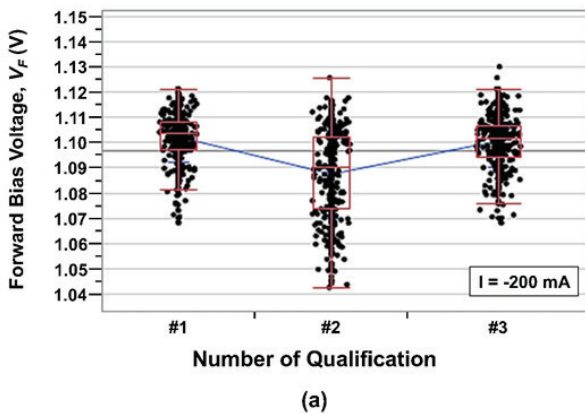


**Figure 8:** Qualification lot electrical distribution when (a)  $V_F$  at 200mA and (b)  $V_R$  at 100  $\mu\text{A}$ .

wafer level electrical test. Based on the 3 qualification lots result shown in Figure 8,  $V_R$  and  $V_F$  electrical test result distribution are well within the specifications. The  $V_F$  distributions are less than 1.5 V and  $V_R$  distribution are above 450 V.

#### 4 Conclusion

In summary, through the understanding of device behaviour and process TCAD simulation performance, the  $W_D$  plays a major role to increase the  $V_R$  when compared to the  $\rho$ . Further, the simulated result is validated through fabricated devices. To achieve beyond 300 V of  $V_R$ , the  $W_D$  is 42  $\mu\text{m}$  and the target  $\rho$  is 32 ohm.cm.

A statistical analysis based on the electrical data was carried out to determine the best wafer substrate window. Subsequently, a validation process using 3 qualification lots is done. The  $V_R$  shows a significant improvement from 300 V to more than 500 V when replaced with the  $W_D$  of 42  $\mu\text{m}$  and the epitaxial resistivity of 32 ohm.cm. The implementations of the new epitaxial specification have been successfully used to expand the product portfolio of this 300V P-i-N power switching diode that can be used in motor control, robotics and power distribution.

#### 5 Acknowledgments

The authors would like to acknowledge all the team members in Institute of Nano Electronic Engineering (INEE), Universiti Malaysia Perlis (UniMAP) for their guidance and help.

#### 6 References

1. M. Quirk and J. Serda, *Semiconductor Manufacturing Technology*. Prentice Hall, 2001.
2. J. E. Ayers, *Digital Integrated Circuits: Analysis and Design*. Taylor & Francis, 2003.
3. S.-M. Kang and Y. Leblebici, *CMOS Digital Integrated Circuits*. Tata McGraw-hill, 2003.
4. B. J. Baliga, *Power Semiconductor Devices*. PWS Publishing Company, 1996.
5. D. A. Neamen, "Semiconductor Materials and Diodes," in *Microelectronics: Circuit Analysis and Design*, McGraw-Hill, 2010, pp. 9–66.
6. J. J. Sparkes, *Semiconductor Devices*, 2, Revised ed. CRC Press, 1994.
7. A. A. Sweet, *Designing Bipolar Transistor Radio Frequency Integrated Circuits*, Illustrate. Artech House, 2007.

8. J. F. White, *Microwave Semiconductor Engineering*, Illustrate. Springer Science & Business Media, 2012.
9. Z. Xu *et al.*, "Fully- and Quasi-Vertical GaN-on-Si p-i-n Diodes: High Performance and Comprehensive Comparison," *IEEE Trans. Electron Devices*, pp. 1–7, 2017.
10. J. Xu, "Technology for Planar Power Semiconductor Devices Package with Improved Voltage Rating Technology for Planar Power Semiconductor Devices Package with Improved Voltage Rating," Virginia Polytechnic Institute and State University, 2008.
11. B. Jayant Baliga, *Fundamental of Power Semiconductor Devices*. Springer, 2008.
12. P. Spirito, *Power Semiconductor Devices*. Dept of Electronics and Telecommunications, University Federico II.
13. C. M. Cheh *et al.*, "The Impacts of Platinum Diffusion to the Reverse Recovery Lifetime of a High Power Diode Devices," *MATEC Web Conf.*, vol. 78, p. 1089, Oct. 2016.
14. C. C. Mee, M. K. Md Arshad, M. Fathil, and U. Hashim, "The effects of intrinsic silicon epitaxial layer in p-i-n diode for high power devices," *ARPJ J. Eng. Appl. Sci.*, vol. 10, no. 18, 2015.
15. R. W. Dutton and A. J. Strojwas, "Perspectives on technology and technology-driven CAD," *IEEE Trans. Comput. Des. Integr. Circuits Syst.*, vol. 19, no. 12, pp. 1544–1560, 2000.
16. J. C. Irvin, "Resistivity of bulk silicon and of diffused layers in silicon," *Bell Syst. Tech. J.*, vol. 41, no. 2, pp. 387–410, 1962.
17. N. I. Shuhaimi *et al.*, "Comparison on I-V performances of Silicon PIN diode towards width variations," in *2010 IEEE International Conference on Semiconductor Electronics (ICSE2010)*, 2010, pp. 12–14.
18. B. Doherty, "PIN Diode Fundamentals," *Microsemi*.
19. W. E. Doherty and R. D. Joos, *The PIN Diode Circuit Designers' Handbook*. Watertown: Microsemi Corporation, 1998.

Arrived: 05. 11. 2016

Accepted: 22. 02. 2017